NASA Technical Memorandum 102321

Development of a High Power Microwave Thruster, With a Magnetic Nozzle, for Space Applications

John L. Power and Randall A. Chapman
Lewis Research Center
Cleveland, Ohio

Prepared for the
24th Microwave Power Symposium
sponsored by the International Microwave Power Institute
Stamford, Connecticut, August 21-23, 1989

DEVELOPMENT OF A HIGH POWER MICROWAVE THRUSTER, WITH A MAGNETIC NOZZLE, FOR SPACE APPLICATIONS

John L. Power and Randall A. Chapman*
National Aeronautics and Space Administration
Lewis Research Center
Cleveland, Ohio 44135

I. SUMMARY

This paper describes the current development of a high-power microwave electrothermal thruster (MET) concept at the NASA Lewis Research Center. Such a thruster would be employed in space for applications such as orbit raising, orbit maneuvering, station change, and possibly translunar or transplanetary propulsion of spacecraft.

The MET concept employs low frequency continuous wave (CW) microwave power to create and continuously pump energy into a flowing propellant gas at relative high pressure via a plasma discharge. The propellant is heated to very high bulk temperatures while passing through the plasma discharge region and then is expanded through a throat-nozzle assembly to produce thrust, as in a conventional rocket engine.

Apparatus, which is described, is being assembled at NASA Lewis to test the MET concept to CW power levels of 30 kW at a frequency of 915 MHz. The microwave energy is applied in a resonant cavity applicator and is absorbed by a plasma discharge in the flowing propellant. The ignited plasma acts as a lossy load, and with optimal tuning, energy absorption efficiencies over 95 percent (based on the applied microwave power) are expected. Nitrogen, helium, and hydrogen will be tested as propellants in the MET, at discharge chamber pressures to 10 atm. This facility will be the first to test the MET concept at these power levels, pressures, and frequency.

The performance of the laboratory MET will be enhanced with a strong solenoidal magnetic field in the throat-nozzle region, a so-called magnetic nozzle. The magnetic field acts to compress the ionized propellant along the thruster axis. This reduces wall impingement and heating and also promotes recombination of the ionic species away from the walls, with the consequent recovery of some of their internal energy. The magnetic nozzle configuration employs a low temperature superconducting magnet with a maximum field strength of up to 6 T, mounted adjacent to the microwave cavity. This is the first known use of a magnetic nozzle to improve the performance of an electrothermal thruster operating at high pressure. (Applied magnetic fields have been extensively used to enhance the operation of low pressure magnetoplasmadynamic (MPD) thrusters.)

Calculations of the predicted performance of the MET are presented. These calculations are made with a two-dimensional kinetics (TDK) computer code normally used for predicting chemical rocket performance. The code has been

E-5017

*NASA-ASEE Faculty Fellow.

extended to include plasma reactions and recently available thermodynamic and kinetic data for hydrogen to temperatures as high as 20 000 K. These are the first known TDK calculations to be made for hydrogen plasmas. The calculations indicate that the MET may reasonably achieve a specific impulse of 2000 sec for hydrogen propellant at a pressure of 10 atm, a temperature of 6000 K, and a power level of 100 kW. The results are in agreement with basic relations for thruster performance. The specific impulse was found to increase with increasing chamber temperature and to depend weakly on chamber pressure, while the thrust was found to be directly proportional to chamber pressure and to depend weakly on chamber temperature.

II. INTRODUCTION

The National Commission on Space emphasized (ref. 1) the necessity of developing high performance advanced propulsion technology in order to accomplish many of the important goals envisaged for the national space program. Electric propulsion is attractive for certain of the proposed missions due to its very high performance.

Electrothermal thrusters are one of three classes of electric propulsion devices, the others being electrostatic and electromagnetic thrusters. Electrothermal thrusters include such types as the arcjet, resistojet, and the laser- or radiofrequency-heated thruster, as well as the microwave thruster. A schematic diagram showing the energy input, use, and loss paths in all such thrusters is presented in figure 1. The input energy, be it deposited in an ac or dc discharge or conveyed by thermal radiation or conduction, heats the flowing propellant to high temperature. The hot propellant then thermodynamically expands via choked flow through a throat and nozzle to produce the device's thrust.

Electrothermal thrusters may in general be operated at relatively high pressures, typically to many atmospheres, and thus can produce relatively high thrust and thrust density levels. In the microwave, arcjet, laser, and radiofrequency thrusters, a plasma discharge is created and maintained by the absorption of the applied electrical or electromagnetic energy. This plasma efficiently heats the propellant gas passing through it or along its boundary. For maximum thruster performance, as much as possible of the energy invested in ionizing, dissociating, and exciting the propellant in the discharge region must be recovered as kinetic energy during the expansion of the hot propellant in the throat and nozzle. The hot plasma species must also be substantially prevented from impinging on the thruster's inside walls, because this is an important wall heating mechanism and energy loss path. The processes by which energy is lost to the walls include electron-ion recombination, atom recombination, convection, conduction, and radiation.

Means for achieving these desirable goals include operating at high pressure, employing a propellant which has fast kinetics for its recombination and de-excitation reactions, constricting the plasma away from the walls, and increasing the concentration of the ionic species along the thruster axis. A promising concept for accomplishing the latter two of these effects is the magnetic nozzle. It is broadly applicable to all types of thrusters producing significant levels of propellant ionization.

Section III of this paper describes specific aspects of MET operation, with particular consideration of operation at high power. It also presents a description of the mechanism and expected effects of a magnetic nozzle, as integrated with the MET. Section IV presents details of the experimental apparatus under assembly at the NASA Lewis Research Center to test the MET at high power levels and with a magnetic nozzle.

In a thermal rocket, the thrust is provided by the choked-flow expansion of the heated propellant or combustion gases through a throat and nozzle. The thrust ideally varies with the chamber pressure as

$$F = C_f A_o P \quad , \tag{1}$$

where C_f is a thrust coefficient, which depends on the propellant gas specific heat ratio and the nozzle expansion ratio, A_o is the minimum throat cross-sectional area, and P is the chamber pressure. This relationship presumes expansion into a vacuum. If C_f remains constant, the thrust should be proportional to the chamber pressure.

The propellant exhaust velocity, v_p, in a thermal rocket is provided by the thermal energy of the heated propellant before expansion. Hence, from kinetic theory, the maximum value of v_p is given by

$$v_p = \left(\frac{3kT}{m_p}\right)^{1/2} \quad , \tag{2}$$

where m_p is the propellant mass per expelled atom, ion, or molecule, k is the Boltzmann constant, and T is the maximum absolute temperature of the expelled species prior to expansion. If only a single propellant species is present, the specific impulse (Isp) will thus be given by

$$Isp = \frac{(3kT/m_p)^{1/2}}{g} \quad , \tag{3}$$

where g is the acceleration due to gravity, showing that the Isp should be proportional to $T^{1/2}$ in this ideal case.

In real thrusters, multiple species are usually present in the expanding propellant. These are all in dynamic, pressure- and temperature-sensitive equilibria with each other and the walls, or only in partial equilibria. In such a case, the calculations of thrust, exhaust velocity, and specific impulse are much more complicated. To enable such calculations, a standardized computer code which predicts and models thermal rocket engine performance has been developed (ref. 2). This two-dimensional kinetics (TDK) code has been used to make the calculations presented in section V, for a wide range of chamber pressures and temperatures with hydrogen as the propellant. These calculations are applicable to the microwave electrothermal thruster.

III. MICROWAVE ELECTROTHERMAL THRUSTER (MET) AND MAGNETIC NOZZLE

A. General Characteristics of the MET

The MET is an electrothermal thruster which employs CW microwave energy to create and maintain a plasma discharge in a flowing propellant so as to heat the propellant. As demonstrated by Arata (ref. 3), such a plasma can be sustained at relative high pressures (>1 atm) and can efficiently heat a propellant gas to temperatures greater than 5000 K, making the concept attractive for propulsion applications. The thruster relies on the choked-flow thermodynamic expansion of the heated propellant through a throat and nozzle to produce thrust. Hence, it possesses the capabilities of high thrust and thrust density (thrust per unit cross-sectional area of the nozzle) common to thermal thrusters operating at high pressure. The major performance (i.e., specific impulse) constraint of such thrusters is throat and nozzle wall material temperature limitations.

The MET possess several potential advantages over other types of electric thrusters. It is electrodeless; hence the erosion and energy losses associated with electric thrusters employing electrodes may be substantially eliminated. The plasma volume can, within limits, be externally controlled in size and location by such variables as the pressure, applied power, gas flow characteristics, and applied magnetic field. Such control of the plasma allows for optimization of the thruster performance which is not available with other types of electric thrusters. The MET can also be operated on a wide variety of propellants.

Very high efficiencies (>95 percent) have been demonstrated by Whitehair (ref. 4) in absorbing the input microwave energy and converting it to propellant kinetic energy in the MET. The input energy is first absorbed by the free electrons in the plasma discharge, and due to the high pressure environment, the electron energy quickly equilibrates with all the propellant species present. Unless the equilibrium plasma temperature becomes high enough to cause significant thermal ionization, the ionization remains quite low - typically less than 1 percent (ref. 5).

B. Applicators

Experimentally, MET evaluation to date has been conducted at the industrial heating frequency of 2450 MHz, with narrow bandwidth power sources. The investigations of Arata (refs. 3 and 6), conducted at 915 MHz in nitrogen and hydrogen, did not employ apparatus intended for thruster evaluation and did not investigate choked flow of the working gas. Two types of microwave applicators, the coaxial and cavity applicators shown in figures 2(a) and (b), respectively, have been successfully employed to achieve efficient energy absorption in the plasma. The coaxial applicator is operated in a transverse electromagnetic (TEM) mode and the plasma discharge acts as an extension of the center conductor. The cavity applicator is operated in a lower order transverse magnetic (TM) mode and the plasma discharge acts as a lossy load. With optimal tuning, efficient coupling of the microwave power into the plasma using both of these applicators has been achieved in nitrogen and helium at low power levels and moderate (1 to 3 atm) pressures (refs. 4 and 7).

When microwave radiation is coupled into a resonant cavity, electromagnetic fields are established in standing wave modes. Energy is absorbed by the plasma through acceleration of the free plasma electrons by the ac electric fields. Thus, the plasma is formed in the region where the electric fields are the strongest. The electrons impart their kinetic energy to the ionic and neutral species in the plasma through collisions. The higher the pressure, the greater the collision frequency and the closer the plasma approaches thermodynamic equilibrium. The cooler propellant gas flowing into and along the periphery of the discharge volume is then heated by convection, conduction, and radiation. These energy transfer processes are generically sketched in figure 1.

The electromagnetic field lines of the TM_{011} and TM_{012} modes are depicted in figures 3(a) and (b). (The subscripts denoting the modes relate to the number of half-wave variations in the azimuthal, radial, and axial components of the electromagnetic field, respectively.) The lower order TM modes of the cavity applicator lend themselves most readily to MET operation because they concentrate the most intense electric fields along the cavity axis, where the plasma discharge is formed. Thus, the plasma is located away from the discharge tube wall and energy losses to the walls are minimized. Stabilization of the plasma volume at a fixed location with a fixed shape is principally the result of the concentration of the electric field on the axis of the cavity and the peripheral cooling of the plasma by the flowing propellant gas and any physical walls present.

Both the TM_{011} and TM_{012} modes have been successfully utilized in cavity applicators (ref. 4) to maintain high-pressure discharges and both will be investigated in the present research effort. The cavity is designed and can be tuned so that either the TM_{011} or TM_{012} mode is singly excited, without admixture of other modes. By adjusting the position of a cavity sliding short and the insertion of the antenna coupling probe, the microwave circuit may be exactly tuned to match the complex impedance of the load and minimize the reflected power from it (ref. 8). The TM_{011} mode is preferable in realizing the MET concept. Not only is the cavity required half as long as that for the TM_{012} mode (which will reduce wall losses), but more importantly the discharge resides at one end of the cavity due to the electric field node at the cavity midpoint. This allows the throat-nozzle assembly to be located outside the cavity, yet still be in close proximity to the discharge which is heating the propellant gas. In this regard, the coaxial applicator (fig. 2(a)) has an advantage over the cavity applicator since the discharge may be placed arbitrarily close to the throat-nozzle assembly.

The MET concept is technically feasible at either the 915 or the 2450 MHz industrial heating frequencies available. In choosing between them to extend investigations to higher power levels than previously attempted, several factors were considered. Some of these relate to the different wavelengths of the microwave radiation at the two frequencies: 33 cm at 915 MHz and 12 cm at 2450 MHz. Cavity, waveguide, and coaxial transmission line dimensions all scale with wavelength. As a result, these components are somewhat heavy and bulky for the lower frequency. However, the larger dimensions allow for larger discharge tubes and throat-nozzle assemblies. This factor may offer both operational and fabrication advantages. Another important consideration is the cost and efficiency of high-power, low ripple magnetron generators at the two frequencies. On both counts, the lower frequency has a distinct

edge. These considerations led to the decision to assemble the apparatus for the present investigation to operate at the 915 MHz frequency.

C. Discharge Characteristics and High-Power Operation

Plasma discharges typically have electron number densities greater than 10^{12} cm^{-3}. At such densities, their cutoff frequency (i.e., plasma frequency) for electromagnetic wave propagation is well above the 915 and 2450 MHz microwave frequencies. The plasma frequency electron number densities at 915 and 2450 MHz are 1.0×10^{10} and 7.5×10^{10} cm^{-3}, respectively. Hence, microwave radiation at either frequency will not propagate through a plasma of even moderate electron density and will instead be mostly reflected at the plasma boundary. Only a small fraction of the energy contained in an electromagnetic wave at these frequencies will be absorbed by the plasma. However, it is the electric fields of the applicators described in the previous section and not the incident electromagnetic waves that transfer the energy to the plasma. This is considered further below.

The quality factor (Q) of a MET resonant cavity is the ratio of the energy stored in the electromagnetic fields to the total energy losses. These losses are to the cavity walls, discharge tube, and plasma. With optimal tuning, the Q approaches 15 000 for an empty cavity and is reduced to less than 100 for a cavity with a plasma load (ref. 9). Hence, the plasma acts as a lossy load and efficiently absorbs the incident microwave power, with the energy losses to the discharge tube and cavity walls being of the order of one percent. As noted above, adjustment of the sliding short position and the insertion of the input power probe provide the capability of exactly tuning the impedance of the plasma load for minimum mismatch and reflected power. Optimal tuning further requires a narrow bandwidth, low ripple microwave signal, which present-day magnetron generators can provide. Ripple and any other oscillating condition causing plasma fluctuations will give rise to an ac component of the plasma load impedance which cannot be accommodated by the dc tuning mechanisms available.

The principal experimental variables affecting and allowing some control of the plasma volume in a MET operating at a fixed frequency are the discharge chamber pressure and the absorbed CW power level. Increasing the pressure compresses the plasma volume, due to increased collision frequencies. Increasing the absorbed power increases the plasma volume, due to increased plasma temperatures and densities. Thus, the plasma volume may be kept roughly constant while increasing the power level by correspondingly increasing the pressure. This is important in achieving high-power operation and permits limited external control of the absorbed power density of the plasma discharge.

Igniting the MET discharge must normally be done at pressures less than 100 torr, to achieve breakdown in the propellant gas. This in turn requires that only modest starting power levels be applied. Otherwise, the discharge, once ignited, will immediately expand to contact the discharge tube walls before the pressure can be raised to prevent this. Such an occurrence could cause melting of the walls and catastrophic failure. With the discharge started at low pressure and power, both variables are simultaneously and smoothly increased to achieve high-power operation. During this process, the cavity must be continually retuned to match the changing load impedance and maintain minimum reflected power operation. At high applied power levels,

even low reflection coefficients mean that substantial and potentially hazardous quantities of power are being reflected back into and absorbed by the microwave circuit.

As the electron density of the plasma is increased, the penetration depth of the electric fields into the plasma is reduced. This is known as the skin effect. At some high level of power density, the skin effect is expected to prevent further increase in the power density. At this point, the plasma density is so high that the microwave power is absorbed in a very thin skin layer and the plasma kinetic pressure is so high that increasing the propellant gas pressure has no further effect in decreasing the plasma volume. Therefore, a further increase of the absorbed microwave power only increases the plasma volume.

The skin effect domination of the MET discharge characteristics at high power may provide a benefit which more than compensates any limits on the plasma power density it imposes. This is that it forces all energy absorption to take place at the plasma boundary, precisely where the desired collisional energy transfer to the cool propellant gas takes place. At the same time, the skin effect protects the hot interior of the plasma from further energy absorption and heating. The result should be a relatively flat temperature profile across the plasma, which will minimize the radiation losses which are expected to constrain high-power operation. Hence, relatively high average plasma temperatures should be achievable for given limiting radiation losses.

During high-power operation, the stability of the MET discharge is of critical concern. Should plasma fluctuations or externally induced perturbations (such as flow instabilities or a microwave generator upset) cause it to extinguish, it may not automatically reignite under the high-pressure conditions prevailing. The cavity will then revert to a mistuned high-Q system. At a high applied power level, discharges may be induced outside the discharge tube or in components of the microwave circuit. Potentially disastrous heating of the cavity walls, discharge tube, or other components could rapidly occur. It is imperative, therefore, that a reflected power or impedance mismatch sensor circuit immediately and automatically shut off the applied microwave signal in the event of a discharge extinction under high power conditions.

D. Magnetic Nozzle

The MET concept lends itself to potentially significant enhancement if implemented with a magnetic nozzle. Figure 4 presents a schematic of such an integrated system, based on a cavity applicator. A strong dc solenoidal magnetic field is configured coaxially with and adjacent to the microwave cavity, with the throat-nozzle assembly situated in the maximum magnetic field region. A magnetic pressure directed in the opposite direction to the magnetic field gradient acts on the charged particles in the plasma and has a magnitude of $B^2/2\mu_o$, where B is the magnetic field strength and μ_o is the permeability of free space. The magnetic pressure is thus about 4 atm at 1 T (10^4 G) and about 140 atm at 6 T (6×10^4 G). If it were possible to heat a diatomic gas at 1 atm to 10 000 K, then fully dissociate and ionize it, the resulting kinetic pressure would be 73 atm. Thus, the magnetic pressure inside present-day superconducting magnets can far exceed the gas kinetic pressure. This illustrates the effective pinching action the dc magnetic field can have on the MET

plasma discharge, an effect which scales as the square of the field strength and is limited only by the available field strength of the magnet employed.

The pinch effect of the magnetic nozzle can serve several useful functions in the MET. By constricting the plasma volume, it may substantially increase the above-described discharge power density limit imposed by the skin effect. It will also directly serve to reduce plasma-wall interactions by compressing the plasma away from the discharge tube walls. (The cyclotron radii of 10 000 K electrons and protons in a 6 T magnetic field are 6.0×10^{-5} and 2.7×10^{-3} cm, respectively.) This effect may substantially ameliorate perhaps the severest limitation to electrothermal thruster performance: that the wall materials cannot survive the propellant temperatures necessary for the desired performance levels. Another benefit of the pinch effect created by the magnetic nozzle is in increasing the recovery of the ionization, dissociation, and excitation energy expended in the discharge volume. The excitation energy resides in the quantum states of the species present. By constricting the charged species along the axis of the thruster, the densities of these species are raised there and the equilibrium and recombination reactions which release the contained energy of these species are thereby promoted. Thus, chemical and electrical energy which would otherwise be lost is converted into the desired kinetic energy.

A final desirable effect of the magnetic nozzle lies in its stabilizing the plasma discharge location on the magnetic field axis. Should the discharge volume asymmetrically expand or move off this axis, due to convective or buoyancy forces for example, the axially symmetric magnetic pressure, which is directed inward, will tend to recenter the discharge volume on the axis and restore its axially symmetric shape. Because of these expected benefits, the apparatus built to test the thruster was designed to incorporate a superconducting magnet forming such a nozzle.

IV. EXPERIMENTAL APPARATUS AND OPERATION

A. Microwave Circuit and Power Generator

The significant components of the microwave circuit to be employed for the MET laboratory testing are shown in figure 5. The circuit is designed to operate at a frequency of 915±5 MHz and at an impedance of 50 Ω. The waveguide section of the system is constructed of standard WR975 waveguide components.

The microwave generator employed is a modified commercial magnetron type with a maximum CW power output of 30 kW. Its output signal has a typical bandwidth of 0.2 MHz. The output power level is adjustable over three ranges (depending on the plate transformer taps connected), providing stable operation from about 2 to 7 kW on the low range, 5 to 12 kW on the middle range, and 7 to 30 kW on the high range. As is characteristic of magnetron generators, the output signal center frequency decreases a few megahertz as the output power is reduced to low levels. No significant sideband radiation is produced by the generator. A 3-port circulator inside the generator protects the tube from injurious back-reflected power. (As seen in fig. 5, a second, external 3-port circulator further protects it.)

Several modifications of the generator electronics circuitry from that of the commercial heating precursor have been implemented to achieve the required

1 percent peak-to-peak ripple specification for the output signal. The principal change is the use of a dual secondary, 3-phase plate transformer with a 12-phase, full-wave rectified output. Other modifications made to reduce the ripple include conversion of the filament heater circuit from ac to dc and the incorporation of substantial additional filtering in both the anode current control and filament heater circuits. In addition, careful balancing of the phase voltages of the input 3-phase, 440 VAC power aids in reducing the ripple.

Although the microwave power applied to the MET cavity can be varied by the generator control, this does not allow the power to be continuously adjusted from a starting level less than 1 kW to an operating level near the 30 kW generator limit. In addition, the few MHz frequency change of the output signal from low to high power complicates maintaining the system tuned for minimum reflected power and impedance mismatch while the magnetron output power is increased. Furthermore, at the low end of each of the power ranges, the output signal is less stable than at the high end.

To overcome these difficulties in continuously adjusting the power applied to the cavity over the full generator range, an external 3-port ferrite circulator and a hybrid phase shifter-tuner are incorporated in the microwave circuit, as seen in figure 5. The 3-port circulator transmits all of the microwave generator output power to the phase shifter-tuner port, with no significant amount of the generator power passing directly to the cavity. The phase shifter-tuner contains double-bucket shorting assemblies. It has one adjustment crank to effect any desired phase shift over a 190° range and another to tune out an impedance mismatch in the system of up to a voltage standing wave ratio of 1.10. By means of these controls, 0 to 98 percent of the input power to the unit can be reflected back into the 3-port circulator and thence to the cavity. The output port of the hybrid phase shifter-tuner leads to a water load with a greater than 30 kW CW power absorption capacity. All of the input power from the generator to the phase shifter-tuner which is not reflected back into the 3-port circulator is absorbed in the water load.

The waveguide-to-coax transition indicated in figure 5 makes a transition from the WR975 waveguide used in the generator and power adjustment section of the microwave circuit to the flexible 12.7 cm (5 in.) coaxial cable used in the remainder of the circuit up to the MET cavity. The transition is specially designed to prevent or minimize moding in the standard 15.6 cm (6-1/8 in.) Electronic Industries Association (EIA) flanged connection to the coax cable. The cutoff frequency in the connector is potentially as low as 876 MHz, somewhat below the 915 MHz operating frequency. Should a small amplitude higher order mode be excited in the coax connector, it will probably damp out completely in the 4.6 m length of the coax cable leading to the MET cavity. However, it remains an undesirable power loss and source of heating in the coax line and connector.

The 12.7 cm flexible coax line has an air dielectric and is rated for approximately 32 kW of CW power at 915 MHz under laboratory conditions. It has a cutoff frequency of about 960 MHz and over its 4.6 m length, it attenuates the 915 MHz signal by less than 0.05 dB.

In conducting an experiment with the MET, it is anticipated that the generator output power level will be set at slightly more that the maximum thruster operating level required, with the phase shifter-tuner set for 0 percent reflection of this power. All of the generator output power will thus be

dumped into the water load (where the power level will be measured accurately by calorimetry). The phase shifter-tuner will then be adjusted to reflect the proper low level of power to the cavity for starting the MET discharge. After the discharge has been started and stabilized, the phase shifter-tuner will be further adjusted to raise the level of power applied to the cavity semi-continuously up to the desired operating level. When this point is reached, only a small fraction of the generator output power will then be absorbed by the water load.

After the MET discharge has been started and frequently while the power to it is being raised, the microwave circuit will be retuned for minimum impedance mismatch and reflected power. Both the tuning adjustments on the cavity and that of the phase shifter-tuner will be used to accomplish this. As previously noted, adjustments of the chamber pressure will also normally be required during the power increase. No adjustment of the output power level of the microwave generator during an experiment is expected to be needed.

B. Microwave Cavity and Discharge Tube

The microwave cavity and discharge tube, as integrated with the superconducting magnet for the magnetic nozzle investigation, are depicted in figure 6. The cavity is a cylinder 45.7 cm in inside diameter by 57.2 cm long. It has a screened viewport located to facilitate visual or spectroscopic observation of the discharge region. The sliding short at the back of the cavity moves on rollers and is driven by a drive and pinion gear arrangement with three lead screws. This mechanism maintains the sliding short always parallel to the fixed front plate of the cavity and prevents it from binding while being moved. The drive gear is manually driven via another gear, enabling fine positioning control and reproducibility with minimal backlash.

The sliding short has a total travel of 24.1 cm, allowing the cavity interior length to be adjusted from 16.5 to 40.6 cm. The calculated approximate shorting locations to tune for the TM_{011} and TM_{012} modes to be investigated are at interior cavity lengths of 19.6 cm and 39.2 cm, respectively. Electrical contact between the shorting flange circumference and the cavity cylindrical wall is maintained during flange translation by beryllium copper fingerstock.

The microwave power input port of the cavity is centered 9.8 cm from the front plate, at the expected location of the downstream electric field maximum in the TM_{011} mode. The 12.7 cm coaxial cable carrying the microwave signal is directly connected to the port via a 15.6 cm (6-1/8 in.) EIA flanged connection. The connectors are modified and the port is designed to maintain the same coaxial cable average dimensions for the outer conductor inner diameter and the inner conductor outer diameter through the connection and port into the cavity itself. Again, this is to preclude the excitation of unwanted higher modes in the unmodified connectors, modes which could then propagate into the cavity and interfere with the clean excitation of the single desired cavity mode.

An extension on the input port center conductor, having a hemispherical end, extends into the cavity and acts as an antenna for the input signal. A captivated threaded ring joining the coupling port and the connector portions of the assembly enables fine tuning adjustment of the excitation probe insertion into the cavity. This insertion may be varied from 2.5 to 5.1 cm,

measured from the cavity inner circumference. Fingerstock attached to the inner circumference of the port outer conductor maintains the proper dimensions and electrical continuity of the outer conductor across the sliding joint at the tuning ring.

The microwave cavity cylindrical body, front flange, sliding short, and coupling port are all fabricated of oxygen-free high conductivity (OFHC) copper. All the interior surfaces of these components are finish-machined and polished to a 0.4 μm finish and then coated with a 100 μm thick layer of silver. This surface treatment is intended not only to assure optimal electrical performance of the cavity but also to make the interior surface highly reflective to the considerable thermal radiation it receives from the discharge tube. All components of the cavity are water-cooled on their exterior, enabling the cavity to absorb the full 30 kW output power of the microwave generator without overheating, in the event of a malfunction in the cavity operation.

The discharge tubes employed in the MET and seen in figure 6 must be fabricated of materials having a high melting point, high strength, and low dielectric loss tangent. The two-tube system shown in the figure extends completely through the cavity and is concentrically positioned on the cavity axis. The outer tube acts as a vacuum containment wall and is fabricated of fused quartz so as to be optically transparent. The inner tube is the actual discharge containment structure. For initial low power testing, it will also be fabricated of fused quartz, enabling spectroscopic and optical observation of the discharge through the cavity viewing port.

Subsequent high-power testing will require an inner discharge tube fabricated of a higher temperature material meeting the other requirements as well. Two good candidates are fused alumina and boron nitride, both of which can withstand working temperatures up to about 2000 °C in nonreactive environments. These are, however, opaque materials, so the discharge produced in these tubes cannot be directly observed through the cavity viewing port. The inner discharge tube initially tested will be 4.7 cm in inner diameter. This dimension may be increased or decreased for subsequent testing, depending on the dimensions and characteristics of the plasma discharge created inside.

The vacuum jacket between the inner and outer discharge tubes will nearly eliminate convective or conductive heat loss radially from the inner tube. Radiative heat loss from it will also be minimized by the transparency of the outer tube and the high reflectivity of the interior surfaces of the cavity. Hence, the inner tube is expected to become quite hot during testing at elevated power levels. This is desirable from the point of view of achieving the best possible thruster performance, because it implies the lowest possible thermal losses. However, with the ultimate goal of testing to discharge pressures as high as 10 atm at power levels up to 30 kW, the material properties of the inner discharge tube will be severely tested, and new and improved tube materials may have to be found.

C. Throat-Nozzle Structure and Magnetic Nozzle

The throat-nozzle structure of the MET laboratory apparatus is attached directly to the end of the inner discharge tube, as seen in figure 6, and is located just outside the microwave cavity front wall. A high-temperature mechanical seal mates the two units together. The throat-nozzle structure is

of one-piece construction, is relatively massive, and will be fabricated of a refractory metal such as tungsten (thoriated), rhenium, or molybdenum. Figure 7 shows the proposed cross-sectional geometry of the structure. The geometry of the throat region is the same as that used for the performance calculations discussed in the next section, including the 1.0 mm throat diameter.

The throat-nozzle structure, as well as the whole front half of the inner discharge tube to which it is attached, will be suspended on the common axis of the microwave cavity and the superconducting magnet by a refractory metal wire fastened to the top of the magnet bore liner. This minimizes the conductive heat loss through the suspension mechanism and allows the assembly to run as hot as possible to achieve maximal thruster performance. The massiveness of the throat-nozzle structure is intended to bring it to a stable equilibrium temperature during steady-state MET testing, a temperature which is insensitive to minor perturbations in the operating parameters. The changes in the structure's steady-state temperature due to changes deliberately made in the experimental conditions are important results to be obtained in the testing. Such temperature changes, for example, directly indicate the magnetic nozzle effect in reducing plasma-wall interaction heating.

The magnetic nozzle is implemented in the experimental apparatus with a superconducting magnet, as shown in figure 6. The magnet is a short solenoid with a clear through-bore and is mounted directly against the front flange of the microwave cavity, with the magnet axis congruent with the cavity and discharge tube axes. Figure 8 is a photograph of the magnet structure with the room temperature bore liner removed, exposing the liquid nitrogen-cooled inner liner and shield. Figure 9 presents a horizontal cross section of the magnet at its midplane. Shown are the liquid helium-cooled coils and shield, the liquid nitrogen-cooled shield, and the room temperature outer shield and flanges. Vacuum jackets separate and insulate all the components at different temperatures. Not shown in figure 9, but indicated in figure 6, is the water-cooled magnet bore liner which completes the room temperature shield through the magnet. Its inner diameter is 7.01 cm and the length of its cylindrical section is 11.6 cm. The bore liner, made of OFHC copper, has a greater than 25 kW cooling capacity and a highly polished interior surface, designed to reflect the maximum possible fraction of the radiant heat reaching it (mainly from the throat-nozzle structure).

The magnetic field map presented in figure 9 shows the strength of the axial field component during maximum field operation. The isostrength contours were derived from detailed field component values calculated for the experimental magnet by a code which takes into account the current flow in the windings as actually constructed. The calculated values have been verified by field measurements. The maximum center line field strength is 5.7 T, though field strengths up to 8 T are found in the NbTi magnet windings. The inductance of the magnet is 7.9 H and the current in the windings at maximum field is 117.3 A.

The magnet power supply enables charging the magnet either under voltage control, at a maximum of 5 V, or at a constant current ramping rate, up to a maximum of 15 A/min. Full charging under the normal current ramp control therefore requires slightly less than 8 min. The power supply also controls the discharging of the magnet, in the same manner and at the same rates as in charging it, by absorbing the magnet's stored energy under controlled conditions. The current flow in the magnet, and hence the magnetic field polarity,

may be automatically reversed. This entails ramping the current down to zero, switching polarity, and ramping the current back up. At full field conditions, slightly less than 16 min, is required to accomplish this. The magnet displays negligible hysteresis, so the field strength is accurately indicated by the current in the windings, whatever the history of the current or field variation.

At any current or field strength up to the maximum, the magnet may be placed in persistent mode operation. This is accomplished by turning off heater power to a superconducting short between the magnet leads, located in the liquid helium-cooled magnet chamber. The current in the magnet windings is thus isolated from that in the power supply circuit, and the latter may be ramped down to zero and the leads to the magnet disconnected, if desired. In persistent mode, the magnet current and field strength show no measurable change or decay with time. The liquid helium and liquid nitrogen consumption rates in persistent mode operation at full field are approximately 170 and 400 cm^3/hr, respectively. The magnet is protected in the event of a quench, during which part or all of the windings suddenly become normal, by the current-carrying capability of the copper matrix in which the NbTi filaments are imbedded when formed as wire for the windings.

The point at which the throat-nozzle structure is suspended from the top of the magnet bore liner is adjustable. As seen from figures 6 and 9, this allows the throat to be placed at the maximum field location in the magnet or, alternatively, either in the converging field upstream of this location or in the diverging field downstream of it. The effects of all these placements on the MET operation - in particular, on the heating of the throat-nozzle structure - will be investigated.

D. Other Experimental Details

The propellant gas feed system for the MET laboratory apparatus is a dual-line system with independent control of the gas flow in each line. One line supplies an axially directed inflow to the discharge tube and the other provides a swirling inflow to it. The gas flow rates in each line are controlled by mass flow controllers which are insensitive to the discharge tube pressure. Nitrogen, helium, and hydrogen, as pure gases, will be investigated in the initial experiments with the MET apparatus, at flow rates up to 25 000 sccm in each channel. The feed system is capable of supplying these flow rates with the discharge tube pressure as high as 10 atm, but initially, this pressure will be controlled at 3 atm, or lower. The gas flow rates, along with the heating of the gas in the discharge tube and throat-nozzle structure, control the discharge tube pressure, because a choked-flow condition is maintained in the throat. In later experiments, two different gases may be run through the gas feed system lines and mixed upon flowing into the discharge tube.

After expanding out through the throat-nozzle structure, the hot propellant gas from the MET apparatus passes through a 30 cm gate valve (shown in fig. 6) and into a large vacuum tank. Figure 10 shows the general configuration of the experimental apparatus and the tank. The tank is approximately 5.8 m long by 3.0 m in diameter. The hot exhaust gas impinges on a liquid nitrogen-cooled cryoliner covering the opposite wall of the tank. The cryoliner acts as a heat exchanger and has adequate liquid nitrogen capacity to

accommodate the full 30 kW power output of the microwave generator. This requires about 5.4 l/min of liquid nitrogen flow.

The exhausted propellant gas, after being cooled by the cryoliner, is then pumped by the vacuum tank's oil diffusion pumps, blower, and roughing pumps. The six diffusion pumps have a maximum total pumping speed of 300 000 l/sec. The blower pumping speed is 2350 l/sec. The tank's pumping performance has been tested with room temperature helium and nitrogen, both with and without the diffusion pumps operating. With the diffusion pumps on, the limiting tank pressure of 5×10^{-4} torr was reached at flow rates of 7000 sccm for helium and 4000 sccm for nitrogen. With the diffusion pumps off, the limiting tank pressure of 0.5 torr was reached at flow rates of 200 000 sccm for helium and 100 000 sccm for nitrogen.

The 0.5 torr tank pressure upper limit does not significantly restrict the MET test operation due to back pressure effects. The discharge tube pressure under such conditions will be greater than 1 atm, or more than 1000 times higher than the back pressure. Hence, the choked flow of the propellant through the throat-nozzle structure should be unaffected. Such back pressures may, however, increase the conductive and convective heat transfer from the inner to the outer discharge tube across the vacuum gap between them. The back pressure may also cause some separation of the exhaust at the downstream end of the nozzle, due to the high exit area ratio (see fig. 7).

Three means have been implemented to stabilize the experimental MET operation and minimize discharge plasma fluctuations. First, the ripple on the input microwave signal has been reduced to a very low level. Second, the applied dc magnetic field from the superconducting magnet will strongly act on and constrain the plasma. Finally, the swirling inflow component of the propellant gas will tend to establish axial symmetry of the gas flow through the discharge tube and maintain a cool gas layer at the wall. These latter two factors should be especially important in overcoming convective and buoyancy effects which have previously been observed (ref. 8) to disturb the axial symmetry of the plasma volume and make it unstable in a horizontal laboratory configuration.

Prior to starting the discharge in the MET apparatus for a typical experiment, swirling inflow of the propellant gas will be introduced and the magnet will be charged to a field strength at least sufficient to stabilize the discharge, when started. The discharge will be ignited and the applied power, propellant flow rate, and discharge tube pressure raised to the desired test levels as previously described. During this process, the microwave cavity and circuit will be continually retuned to minimize reflected power.

When the desired test conditions are reached, the magnetic field, the total propellant flow rate, and the split of the gas inflow between axial and swirl components may be varied. Actual test conditions of propellant flow rate, discharge tube pressure, and applied power will be defined on the basis of the performance calculations described in the following section. When an experiment is concluded and the microwave power turned off, the propellant flow will typically be left unchanged until the discharge tube and throat-nozzle structure have cooled down to room temperature, at which point a cold flow measurement of the discharge tube pressure will be taken. The hot and cold pressure measurements at constant flow allow calculations to be made of

the ideal thrust, specific impulse, and energy efficiency for the experimental conditions (ref. 8).

Simple diagnostics will initially be employed to characterize the MET operating conditions and performance. The microwave generator output power will be measured calorimetrically in the water load attached to the hybrid phase shifter-tuner while no power is applied to the cavity. The power dumped into the water load will also be frequently measured while the discharge is in operation. With the reflected power known from reading the sensor connected to the reflected power port of the in-line dual directional coupler (see fig. 5), accurate measurements of the microwave power transmitted to and absorbed in the cavity will always be available. A less accurate measurement of the power transmitted to the cavity is also provided by the sensor connected to the forward power port of the dual directional coupler.

All the other cooling circuits in the experimental apparatus will also be instrumented for calorimetric measurements. This applies as well to the cryoliner heat exchanger in the vacuum tank. Its liquid nitrogen usage rate and outlet temperature approximately measure the collected thruster exhaust beam power. At the elevated power levels of the intended testing, all of the above calorimetric measurements should be quite accurate. With sufficiently complete calorimetric data from all the cooling circuits and sufficiently low losses in the uncooled components of the apparatus, an energy balance may be constructed giving an estimate of the thruster thermal efficiency and all of its energy loss paths.

Other diagnostics measure the discharge chamber pressure and provide the propellant flow rates in both channels of the gas feed system. The dc magnetic field strength as a function of location is given by the magnet current, in conjunction with the field map.

The equilibrium temperatures of the throat and nozzle of the throat-nozzle structure will be obtained via optical pyrometry. These measurements should reveal and quantify any magnetic nozzle effect in reducing plasma-wall interactions in these regions. A pyrometer will also be employed through the cavity viewport to observe the inner discharge tube exterior surface (and the discharge itself in the case of a fused quartz inner tube). Data from these observations will give the temperature distribution along the inner discharge tube in the region of the discharge. When opaque inner tubes are employed, this data will be particularly valuable in determining the location and extent of the plasma discharge.

In later experiments, additional and more sophisticated diagnostics will be implemented to better characterize the performance and properties of the thruster. These include the use of emission spectroscopy and other noninvasive diagnostics to measure the concentrations and temperatures of the various species in the discharge region, as well as in the throat and nozzle regions. Of equal importance, a direct thrust measurement system is planned. This will provide experimental thrust measurements which also will give values for the specific impulse (Isp). These experimentally determined values should be of much improved reliability compared with the calculated ideal values obtained from measurements of the hot and cold discharge chamber pressure at constant flow rate.

V. CALCULATED PROPULSION PERFORMANCE CHARACTERISTICS

The propulsion performance characteristics of the MET thruster have been predicted with hydrogen as the propellant. These calculations were made with a two-dimensional kinetics (TDK) computer code usually used for predicting chemical rocket performance. The code was extended to include reactions involving electrons, ions, and third bodies. These are the first known TDK calculations for hydrogen plasma flow through a nozzle. Previous efforts have been limited to one-dimensional kinetics (ODK) calculations (ref. 10). The code utilizes recently calculated high-temperature (up to 20 000 K) thermodynamic data for hydrogen (ref. 11). It also computes performance characteristics for one-dimensional frozen flow (ODF), one-dimensional equilibrium (ODE), and one-dimensional kinetics (ODK) analyses. The reaction rates used in the kinetics calculations are given in table I (ref. 10). Results of these computations are applicable to all electrothermal propulsion concepts utilizing hydrogen propellant.

The initial conditions for all the calculations assume thermodynamic equilibrium in the chamber region for a given temperature or enthalpy at an assigned pressure. The equilibrium conditions are calculated by the chemical equilibrium code (CEC) subprogram. The ODF calculations then are made assuming that the thermodynamic equilibrium concentrations of the various species in the chamber are maintained during expansion through the nozzle (i.e., the specie concentrations are frozen at the chamber conditions). The ODE calculations are made assuming that thermodynamic equilibrium is reestablished at every point throughout the expansion process. The ODK calculations use the reaction rates to obtain better estimates of the specie concentrations during expansion through the nozzle. The TDK calculations also use the reaction rates to obtain estimates of the specie concentrations during expansion and compute the performance losses due to the geometry of the chamber-throat-nozzle walls. The method of characteristics is employed in the TDK calculations to compute the properties of the expanding propellant along streamlines which span the throat-nozzle volume. The chamber-throat-nozzle assembly geometry parameters used are shown in figure 11. The actual values employed for these parameters closely describe the throat region of the chamber-throat-nozzle structure depicted in figure 7, including the 1 mm inner diameter throat. All of the results presented here are for a subsonic or contraction (chamber-to-throat) area ratio of 5 and a supersonic or expansion (nozzle-to-throat) area ratio of 75.

The ODE results give the upper bound on the performance, because the maximum amount of excitation, dissociation, and ionization energy in the propellant species is recovered while thermodynamic equilibrium is maintained throughout the propellant expansion and cooling in the nozzle. The ODF results, on the other hand, give the lower bound on the performance, because none of the above types of nonkinetic energy are recovered during expansion. The ODK results are always intermediate between the other two and reflect the extent to which the nonkinetic energy is actually recovered. The TDK results, which are the most realistic, are slightly lower than the ODK results since they take into account the losses due to the throat-nozzle wall curvature during expansion.

The vacuum specific impulse as a function of chamber temperature at a chamber pressure of 10 atm is given in figure 12. The specific impulse shows roughly the $T^{1/2}$ dependence on temperature predicted by equation (3). The

I_{sp} was found to depend weakly on the chamber pressure. The results shown in the figure indicate that a specific impulse of 2000 sec can be reached for a chamber temperature of about 6000 K. Increasing the chamber temperature from 6000 K to 12 000 K does not gain much improvement in the specific impulse. This is due the fact that increasing the enthalpy, in this range, results in increased ionization, not greater kinetic energy, of the hydrogen in the chamber, and little of the ionization energy is recovered during the expansion process. The specific impulse from the kinetics calculations is seen in figure 12 to be near the equilibrium limit at the lower temperatures and near the frozen flow limit at the higher temperatures, again indicating the extent to which the ionization energy is not recovered during expansion.

The thrust as a function of chamber pressure at a chamber temperature of 4000 K is shown in figure 13. The thrust is seen to be directly proportional to the pressure, in agreement with equation (1), and was found to depend weakly on the chamber temperature. The thrust and specific impulse tradeoff at a constant power (i.e., input enthalpy) of 107 kW is shown in figure 14. This relationship agrees with the basic propulsion relation which predicts that specific impulse and thrust are inversely proportional to each other. This tradeoff provides a valuable capability for electrothermal thrusters: high thrust levels may be obtained at the expense of specific impulse by increasing the propellant mass flow rate.

The results shown in figures 12 to 14 do not include plasma-wall interactions, which will lower the performance of the MET. Such interactions include electron-ion and atom-atom recombination, heat conduction and convection, and radiation transfer. The MET experimental apparatus described in the previous sections includes several features, such as the magnetic nozzle, which are designed to reduce these wall interactions. When the wall interactions are sufficiently reduced, the experimental results are expected to approach the TDK predicted performance for the throat-nozzle configuration tested, taking into account boundary layer losses.

VI. CONCLUDING REMARKS

This paper describes the microwave electrothermal thruster (MET) concept and apparatus being assembled at the NASA Lewis Research Center to test it. It also presents the predicted MET performance as calculated using a thermal rocket performance computer code. The laboratory apparatus is designed to operate at 915 MHz and at CW power levels up to 30 kW. This type of thruster has not previously been evaluated at frequencies below 2450 MHz or at power levels more than about 10 percent of that intended in this investigation.

In the MET laboratory apparatus, the microwave energy is applied in a cavity applicator and is absorbed by a plasma discharge in the flowing propellant. The TM_{011} and TM_{012} standing wave modes will be employed in the testing. They concentrate the electric field on the cavity axis where the discharge is desired. A low ripple microwave signal is required to minimize plasma fluctuations and tuning losses. The ignited plasma acts as a lossy load, and, because of this, energy absorption efficiencies greater than 95 percent are expected.

The plasma discharge is started at low power and pressure, and then both variables are smoothly and simultaneously raised to the operating levels. This keeps the plasma volume controlled and roughly constant in size. During the

the power increase, the cavity must be continually retuned to minimize reflected power in the system. The power applied to the cavity is principally varied by means of a hybrid phase shifter-tuner in the microwave circuit. The propellant gases to be tested are nitrogen, helium, and hydrogen, at discharge chamber pressures up to 10 atm and flow rates initially up to 50 000 sccm.

A magnetic nozzle is incorporated in the experimental apparatus and is expected to significantly improve the MET performance. The magnetic nozzle is created by a short, solenoidal superconducting magnet generating a maximum on-axis field strength of 5.7 T, applied in the throat-nozzle region. The pinch effect and high magnetic pressures generated by the magnetic field have the potential to reduce wall losses from the hot plasma species; promote recovery of ionization, dissociation, and excitation energy from the hot species; and stabilize the plasma discharge in the cavity. The stabilizing effect of the magnetic field on the plasma will be augmented fluid-dynamically by the use of a swirl component in the propellant flow.

The skin effect, which limits microwave energy absorption to the outermost layer of a dense plasma discharge, is expected to play a major role in the high power operation of the MET. This effect may limit the achievable power densities in the plasma discharge but it also is expected to yield a uniform temperature profile across the plasma volume, with the energy absorption taking place at the plasma surface where the energy must be transferred to the surrounding unheated propellant. Radiation losses from the plasma should be minimized by this mechanism. The magnetic field of the magnetic nozzle is expected to compress the plasma volume beyond the skin effect limit, thus permitting higher power density operation of the MET.

The propulsion performance of the MET with hydrogen propellant has been predicted with a two-dimensional kinetics (TDK) computer code which incorporates one-dimensional equilibrium (ODE), one-dimensional frozen flow (ODF), and one-dimensional kinetics (ODK) subprograms. The ODE results give the upper bound on the performance, in which the maximum amount of the excitation, dissociation, and ionization energy invested in the propellant in the discharge chamber is recovered as it expands and cools in the nozzle. The ODF results give the lower bound on the performance, in which none of the above types of nonkinetic energy is recovered during expansion. The ODK results are intermediate between the other two and reflect the extent to which the nonkinetic energy actually is recovered. The TDK results, which are the most realistic, are lower than the ODK results and take into account the losses due to the throat-nozzle geometry during expansion.

The specific impulse was found from the TDK calculations to increase approximately as the square root of the chamber temperature and to depend weakly on the chamber pressure. A specific impulse of 2000 sec is achievable by the MET with a bulk gas chamber temperature of 6000 K, at a chamber pressure of 10 atm. The thrust was found to be directly proportional to the chamber pressure and to depend weakly on the chamber temperature.

The TDK calculations to date have not taken into account wall losses due to recombination and thermal heating effects. The MET experimental apparatus is designed to minimize these losses, by such means as the magnetic nozzle. When the wall interactions are sufficiently reduced, the experimental results are expected to approach the performance predicted by the full TDK code.

REFERENCES

1. Pioneering the Space Frontier, U.S. National Commission on Space, Bantam Books, New York, 1986.

2. Nickerson, G.R., et al.: Two-Dimensional Kinetics (TDK) Nozzle Performance Computer Program, Software and Engineering Associates, Inc., Carson City, NV, February, 1988.

3. Arata, Y.; Miyake, S.; and Kobayashi, A.: High Power Microwave Discharge in Atmospheric Hydrogen Gas Flow. J. Phys. Soc. Japan, vol. 44, no. 3, Mar. 1978, pp. 998-1003.

4. Whitehair, S.; Asmussen, J.; and Nakanishi, S.: Microwave Electrothermal Thruster Performance in Helium Gas. J. Propulsion Power, vol. 3, no. 2, Mar.-Apr. 1987, pp. 136-144.

5. Chapman, R.: Energy Distribution and Transfer in Flowing Hydrogen Microwave Plasmas. Ph.D. Thesis, Michigan State Univ., 1986.

6. Arata, Y., et al.: Research of a Stationary High Power Microwave Plasma at Atmospheric Pressure. J. Phys. Soc. Japan, vol. 40, no. 5, May 1976, pp. 1456-1461.

7. Asmussen, J; and Whitehair, S.: Experiments and Analysis of a Compact Electrothermal Thruster. IEPC Paper 88-101, Oct. 1988.

8. Whitehair, S.: Experimental Development of a Microwave Electrothermal Thruster. Ph.D. Thesis, Michigan State Univ., 1986.

9. Frasch, L.L.: An Experimental and Theoretical Study of a Microwave Cavity Applicator Loaded with Lossy Materials. Ph.D. Thesis, Michigan State Univ., 1987.

10. McCay, T.D.; and Dexter, C.E.: Chemical Kinetic Performance Losses for a Hydrogen Laser Thermal Thruster. J. Spacecr. Rockets, vol. 24, no. 4, July-Aug. 1987, pp. 372-376.

11. McBride, B.J.: Personal Communication, NASA Lewis Research Center, Cleveland, OH, 1988.

TABLE I. - HYDROGEN REACTIONS AND KINETIC DATA

[M is a third body; k is the reaction rate, with units of cm^3, K, mole, and sec; hν is a photon.]

Reaction	Reaction rate
$H + H + M \longrightarrow H_2 + M$	$k = 6.40 \times 10^{17}\ T^{-1.0}$
$H^+ + e^- + M \longrightarrow H + M$	$k = 5.26 \times 10^{26}\ T^{-2.5}$
$H_2 + e^- \longrightarrow H + H + e^-$	$k = 1.91 \times 10^{11}\ T\ e^{(-102.T)}$
$H^- + H \longrightarrow H_2 + e^-$	$k = 7.83 \times 10^{14}$
$H^+ + e^- \longrightarrow H + h\nu$	$k = 3.77 \times 10^{13}\ T^{-0.58}$
$H^+ + 2e^- \longrightarrow H + e^-$	$k = 7.08 \times 10^{39}\ T^{-4.5}$
$H^+ + H^- \longrightarrow H + H$	$k = 1.30 \times 10^{18}\ T^{-0.5}$

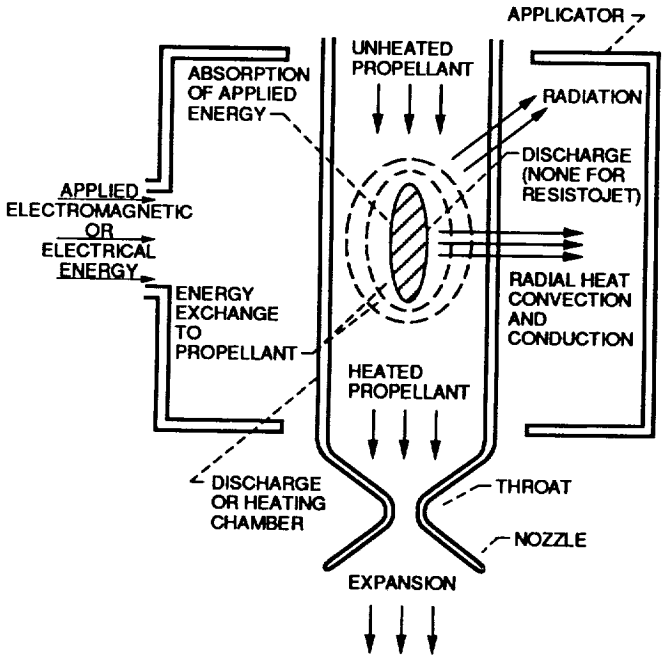

Figure 1. - Electrothermal thruster schematic.

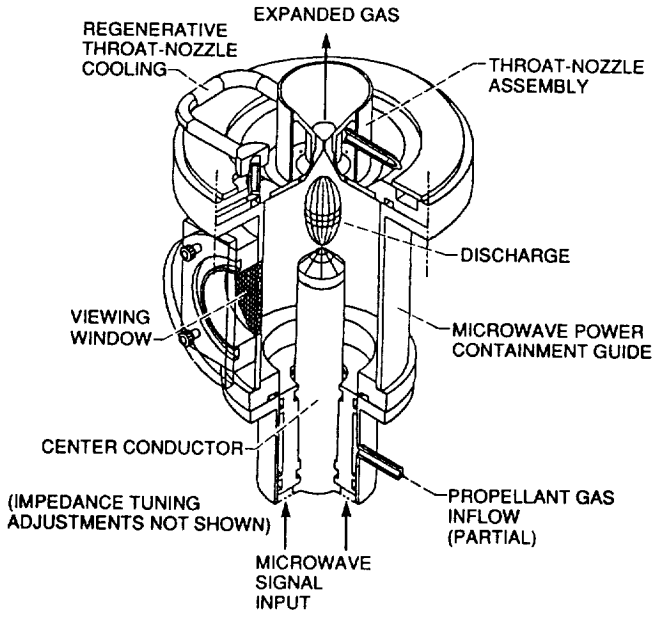

(a) Coaxial.

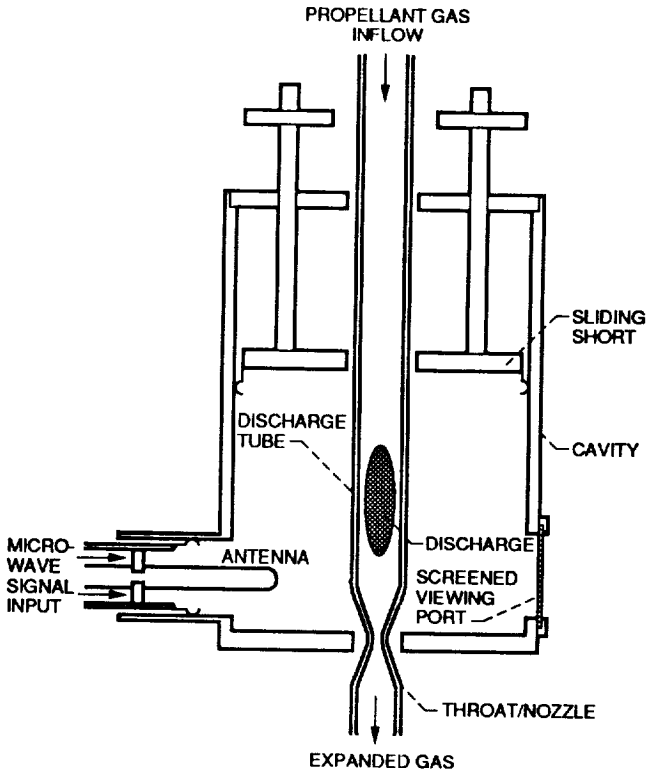

(b) Cavity.

Figure 2. - Microwave thruster applicators.

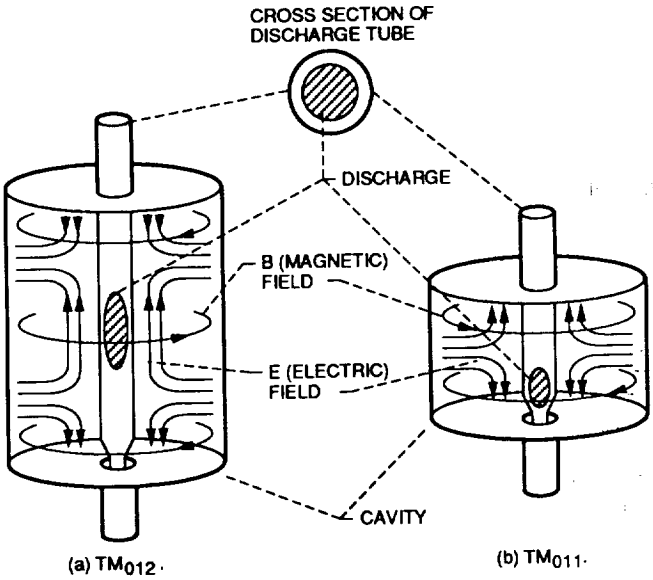

Figure 3. - Electromagnetic field patterns for MET modes, with discharge placement.

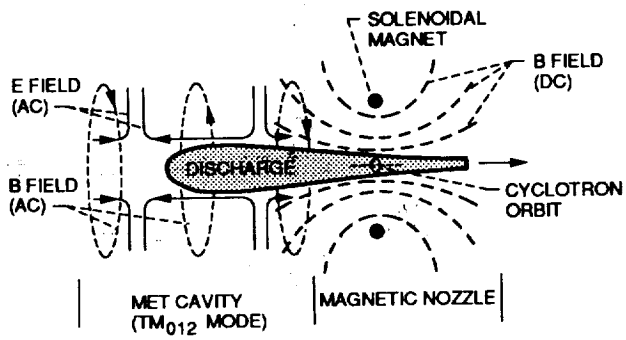

Figure 4. - Magnetic nozzle schematic, as integrated with cavity-MET.

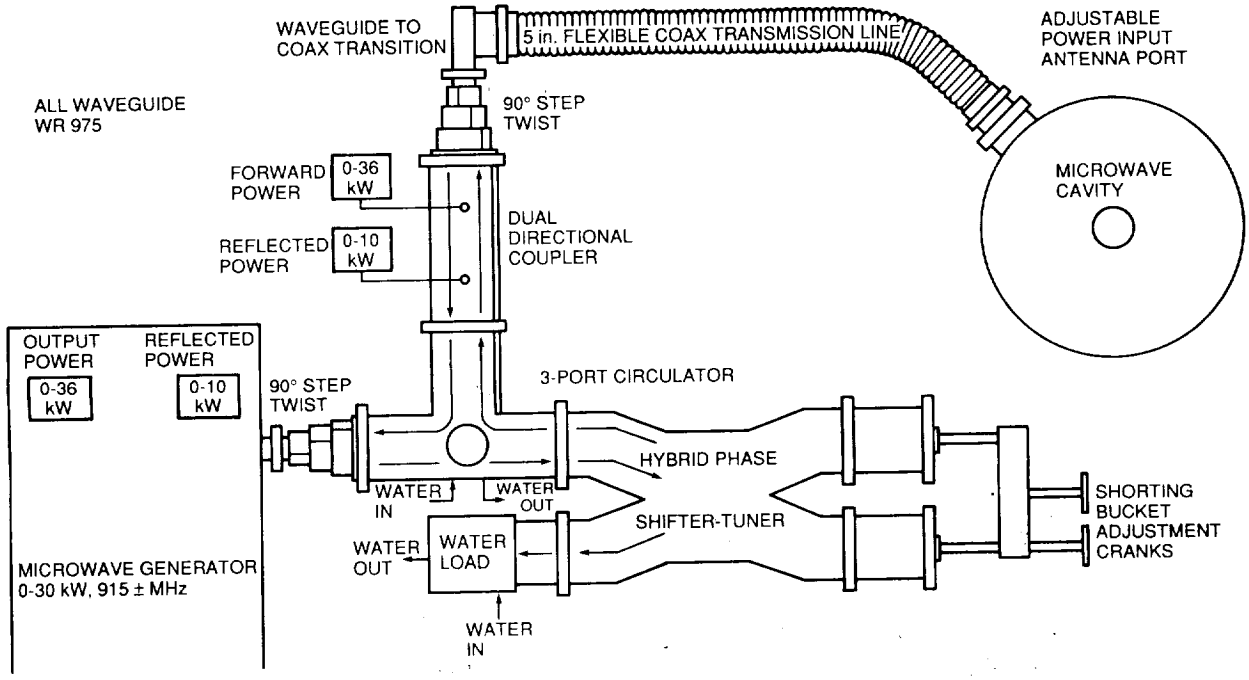

Figure 5. - Microwave circuit for MET test apparatus.

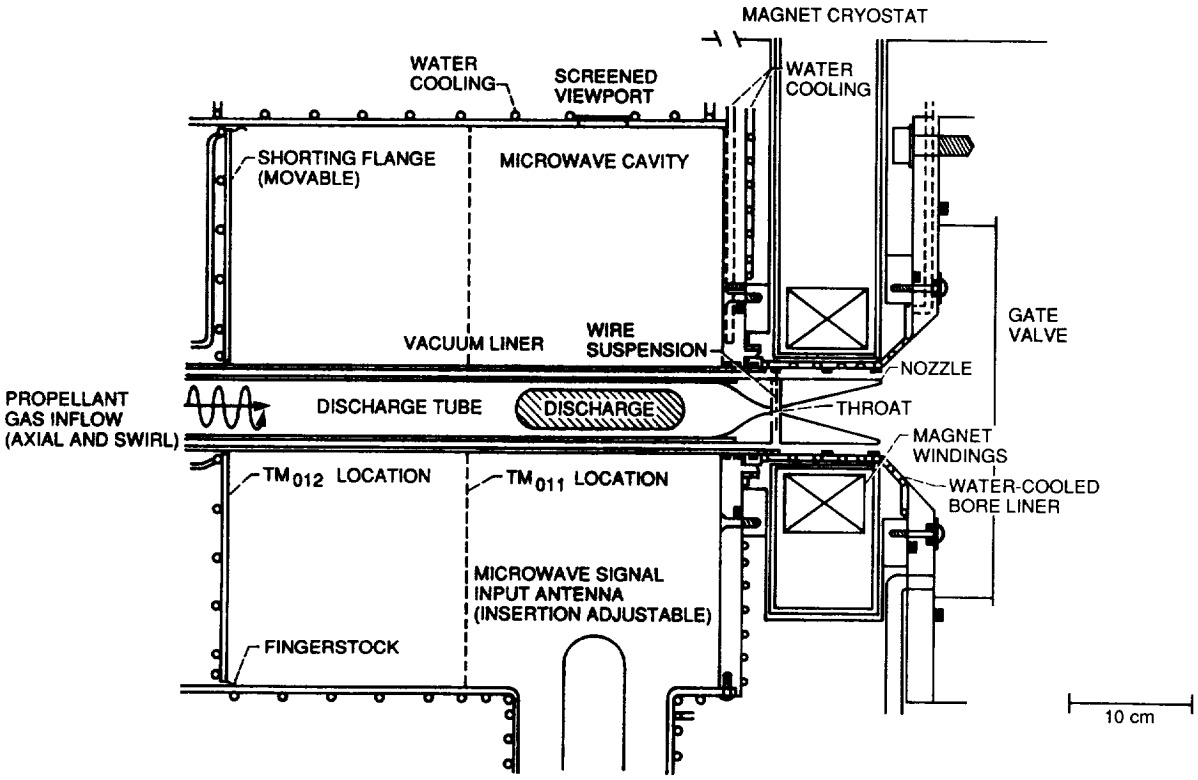

Figure 6. - Cavity-MET apparatus integrated with superconducting magnet.

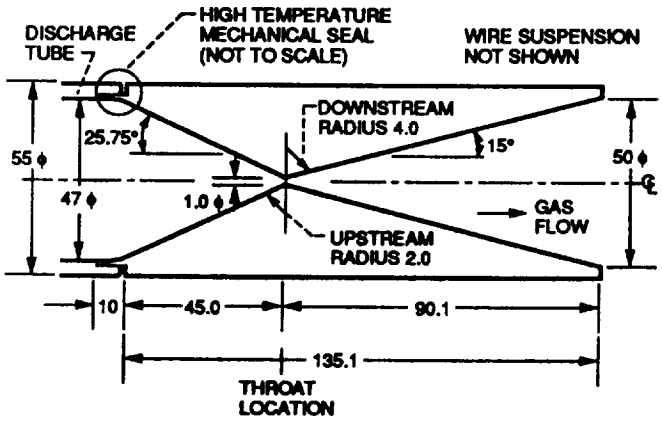

Figure 7. - Throat-nozzle structure geometry. (Dimensions in millimeters)

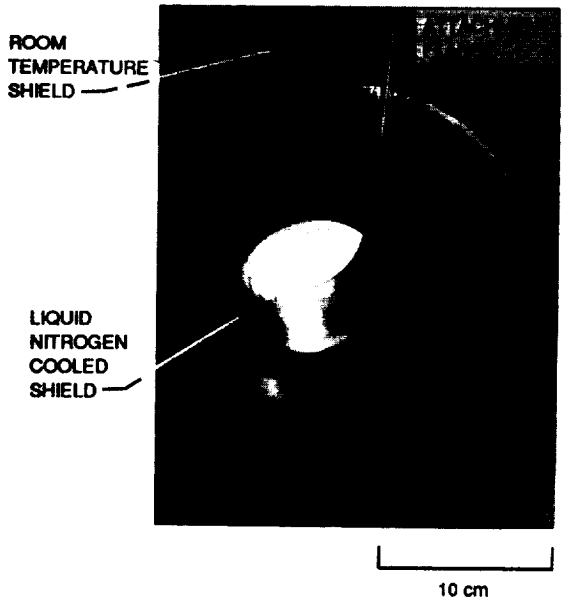

Figure 8. - Superconducting magnet.

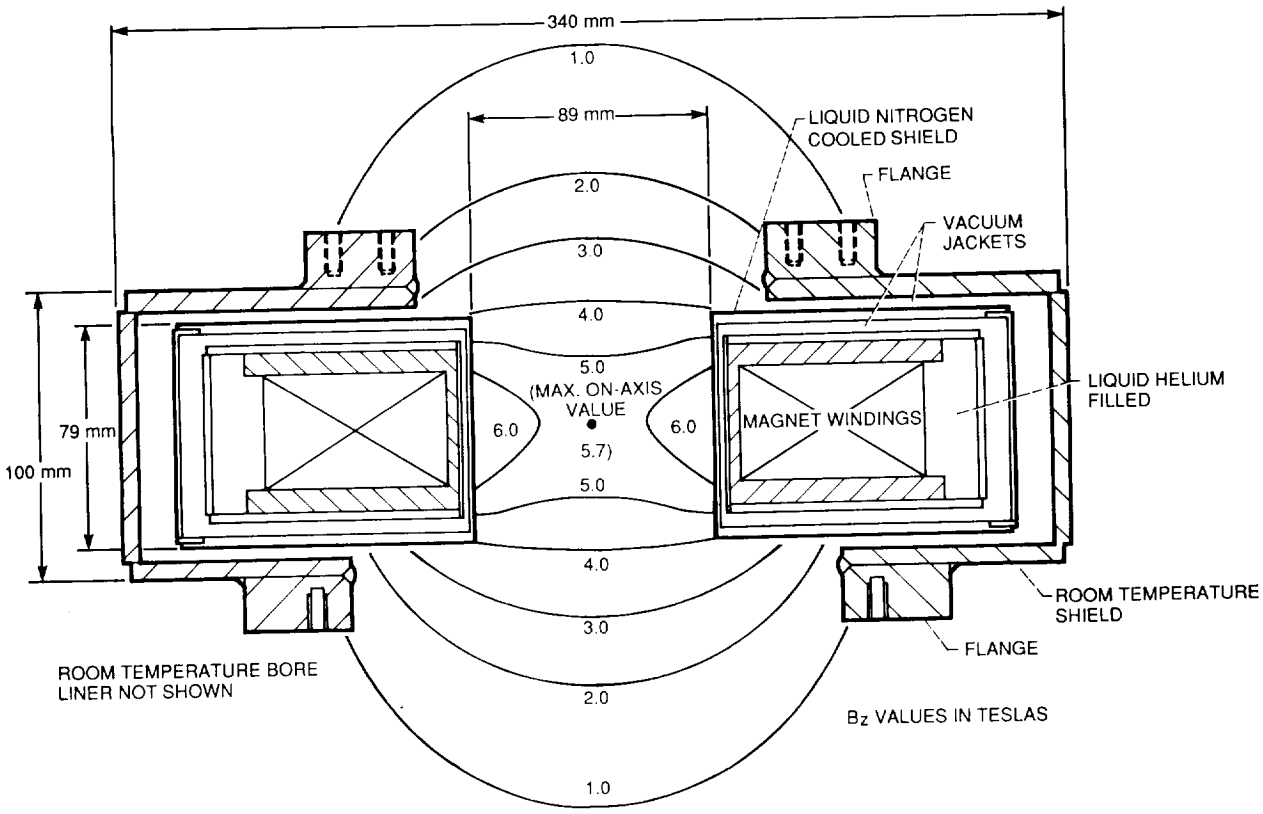

Figure 9. - Cross section and axial component field strength map of superconducting magnet.

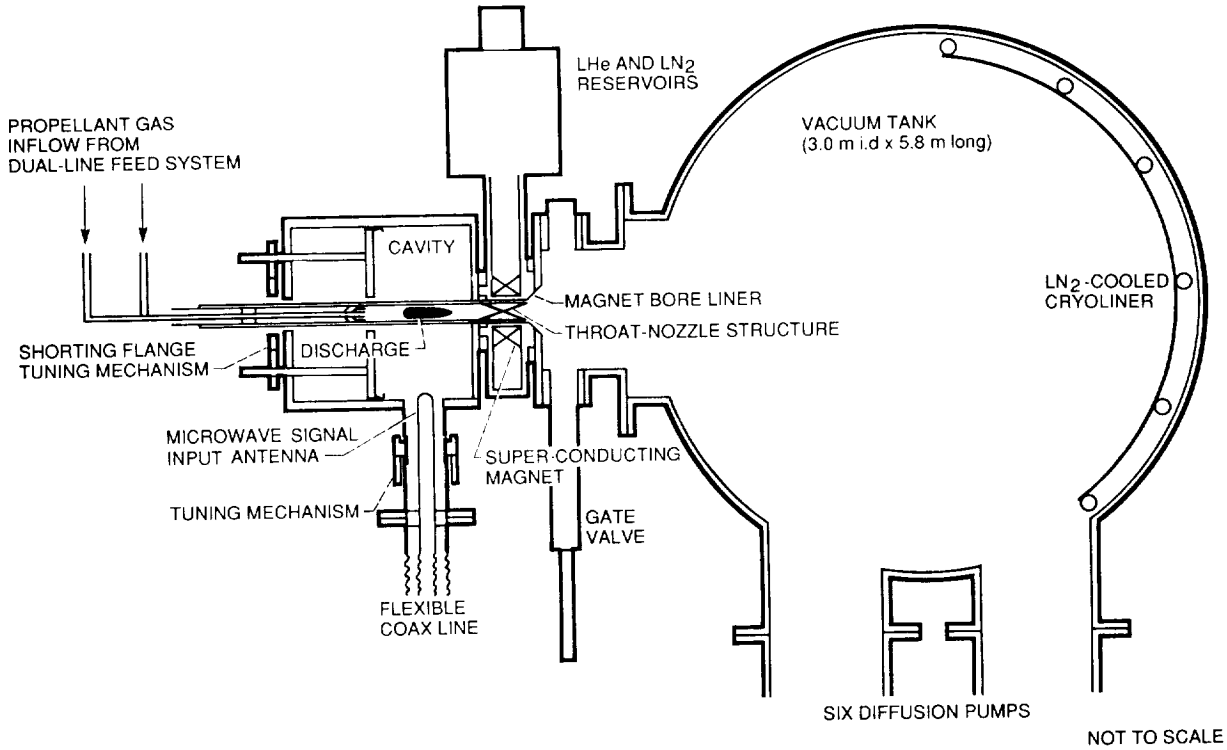

Figure 10. - Microwave electrothermal thruster test apparatus and vacuum facility.

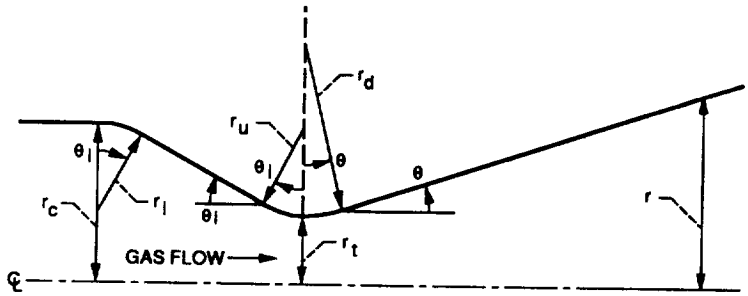

$\theta_l = 25°$ THROAT RADIUS (r_t) = 1 mm
$\theta = 15°$
$r_l = 2$ mm CHAMBER AREA RATIO $(r_c/r_t)^2 = 5$
$r_d = 4$ mm
$r_u = 2$ mm EXPANSION AREA RATIO $(r/r_t)^2 = 75$

Figure 11. - Chamber-throat-nozzle assembly geometry for TDK calculations.

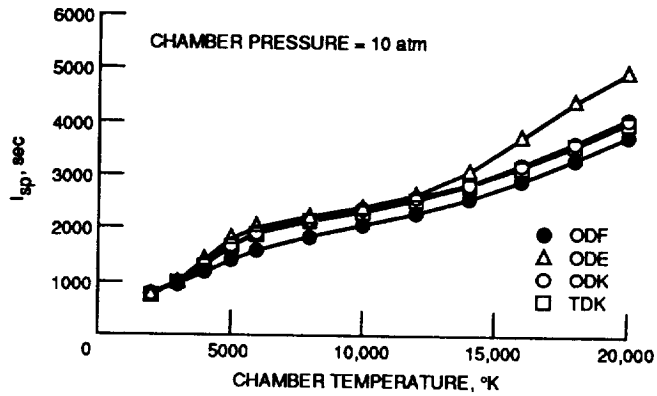

Figure 12. - Specific impulse as a function of chamber temperature.

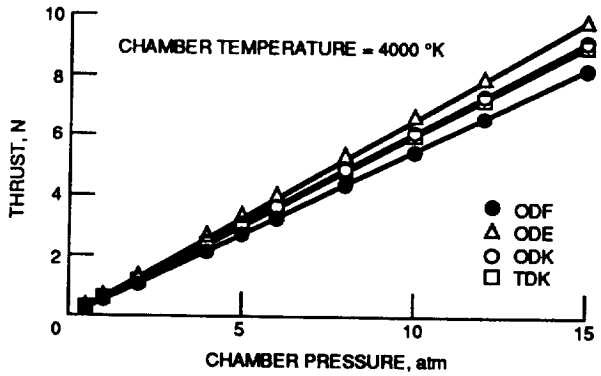

Figure 13. - Thrust as a function of chamber pressure.

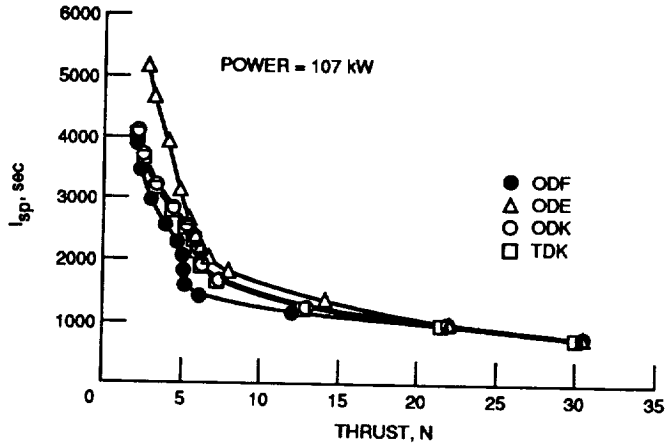

Figure 14. - Isp and thrust tradeoff at constant power.

NASA
National Aeronautics and Space Administration

Report Documentation Page

1. Report No.	2. Government Accession No.	3. Recipient's Catalog No.
NASA TM-102321		

4. Title and Subtitle	5. Report Date
Development of a High Power Microwave Thruster, With a Magnetic Nozzle, for Space Applications	6. Performing Organization Code

7. Author(s)	8. Performing Organization Report No.
John L. Power and Randall A. Chapman	E-5017
	10. Work Unit No. 506-42-31

9. Performing Organization Name and Address	11. Contract or Grant No.
National Aeronautics and Space Administration Lewis Research Center Cleveland, Ohio 44135-3191	13. Type of Report and Period Covered Technical Memorandum

12. Sponsoring Agency Name and Address	14. Sponsoring Agency Code
National Aeronautics and Space Administration Washington, D.C. 20546-0001	

15. Supplementary Notes

Prepared for the 24th Microwave Power Symposium sponsored by the International Microwave Power Institute, Stamford, Connecticut, August 21-23, 1989. Randall A. Chapman, NASA/ASEE Faculty Fellow.

16. Abstract

This paper describes the current development of a high-power microwave electrothermal thruster (MET) concept at the NASA Lewis Research Center. Such a thruster would be employed in space for applications such as orbit raising, orbit maneuvering, station change, and possibly trans-lunar or trans-planetary propulsion of spacecraft. The MET concept employs low frequency continuous wave (CW) microwave power to create and continuously pump energy into a flowing propellant gas at relative high pressure via a plasma discharge. The propellant is heated to very high bulk temperatures while passing through the plasma discharge region and then is expanded through a throat-nozzle assembly to produce thrust, as in a conventional rocket engine. Apparatus, which is described, is being assembled at NASA Lewis to test the MET concept to CW power levels of 30 kW at a frequency of 915 MHz. The microwave energy is applied in a resonant cavity applicator and is absorbed by a plasma discharge in the flowing propellant. The ignited plasma acts as a lossy load, and with optimal tuning, energy absorption efficiencies over 95 percent (based on the applied microwave power) are expected. Nitrogen, helium, and hydrogen will be tested as propellants in the MET, at discharge chamber pressures to 10 atm. This facility will be the first to test the MET concept at these power levels, pressures, and frequency. The performance of the laboratory MET will be enhanced with a strong solenoidal magnetic field in the throat-nozzle region, a so-called "magnetic nozzle". The magnetic field acts to compress the ionized propellant along the thruster axis. This reduces wall impingement and heating and also promotes recombination of the ionic species away from the walls, with the consequent recovery of some of their internal energy. The magnetic nozzle configuration employs a low temperature superconducting magnet with a maximum field strength of up to 6 T, mounted adjacent to the microwave cavity. This is the first known use of a magnetic nozzle to improve the performance of an electrothermal thruster operating at high pressure. (Applied magnetic fields have been extensively used to enhance the operation of low pressure magnetoplasmadynamic (MPD) thrusters.) Calculations of the predicted performance of the MET are presented. These calculations are made with a two-dimensional kinetics (TDK) computer code normally used for predicting chemical rocket performance. The code has been extended to include plasma reactions and recently available thermodynamic and kinetic data for hydrogen to temperatures as high as 20 000 K. These are the first known TDK calculations to be made for hydrogen plasmas. The calculations indicate that the MET may reasonably achieve a specific impulse of 2000 sec for hydrogen propellant at a pressure of 10 atm, a temperature of 6000 K, and a power level of 100 kW. The results are in agreement with basic relations for thruster performance. The specific impulse was found to increase with increasing chamber temperature and to depend weakly on chamber pressure, while the thrust was found to be directly proportional to chamber pressure and to depend weakly on chamber temperature.

17. Key Words (Suggested by Author(s))	18. Distribution Statement
Microwave; Thruster; Electrothermal; Electric propulsion; Magnetic nozzle; Plasma	Unclassified – Unlimited Subject Category 20

19. Security Classif. (of this report)	20. Security Classif. (of this page)	21. No of pages	22. Price*
Unclassified	Unclassified	26	A03

*For sale by the National Technical Information Service, Springfield, Virginia 22161